

Raman-induced polarization stabilization of vector solitons in circularly birefringent fibers

N. Korneeov,¹ E.A. Kuzin,^{1,*} B. A. Villagomez-Bernabe,¹ O. Pottiez,² B. Ibarra-Escamilla,¹ A. González-García,¹ and M. Durán-Sánchez

¹Instituto Nacional de Astrofísica Óptica y Electrónica INAOE, Luis E. Erro, No. 1, C. P. 72824, Tonantzintla, Puebla, Pue. México

²Centro de Investigaciones en Óptica, Loma del Bosque No. 115, Col. Lomas del Campestre, León, Gto., 37150, México

*ekuz@inaoep.mx

Abstract: Vector soliton propagation in circularly birefringent fibers was studied by perturbation analysis and numerically. The results show that in presence of both Raman self-frequency shift and group velocity difference between circularly polarized components the Raman cross-polarization term causes an energy transfer from the slower to the faster circular component of vector solitons. This effect leads to polarization stabilization of circularly polarized vector solitons.

©2012 Optical Society of America

OCIS codes: (060.4370) Nonlinear optics, fiber; (060.5530) Pulse propagation and temporal solitons.

References and links

1. L. F. Mollenauer, R. H. Stolen, and J. P. Gordon, "Experimental observation of picoseconds pulse narrowing and solitons in optical fiber," *Phys. Rev. Lett.* **45**(13), 1095–1098 (1980).
2. G. P. Agrawal, *Nonlinear Fiber Optics* (Academic Press, 2001).
3. C. R. Menyuk, "Stability of solitons in birefringent optical fibers. I: Equal propagation amplitudes," *Opt. Lett.* **12**(8), 614–616 (1987).
4. C. R. Menyuk, "Stability of solitons in birefringent optical fibers. II. Arbitrary amplitudes," *J. Opt. Soc. Am. B* **5**(2), 392–402 (1988).
5. D. N. Christodoulides and R. I. Joseph, "Vector solitons in birefringent nonlinear dispersive media," *Opt. Lett.* **13**(1), 53–55 (1988).
6. M. N. Islam, C. D. Poole, and J. P. Gordon, "Soliton trapping in birefringent optical fibers," *Opt. Lett.* **14**(18), 1011–1013 (1989).
7. N. N. Akhmediev, A. V. Buryak, J. M. Soto-Crespo, and D. R. Andersen, "Phase-locked stationary soliton states in birefringent nonlinear optical fibers," *J. Opt. Soc. Am. B* **12**(3), 434–439 (1995).
8. S. T. Cundiff, B. C. Collings, and W. H. Knox, "Polarization locking in an isotropic, modelocked soliton Er/Yb fiber laser," *Opt. Express* **1**(1), 12–21 (1997).
9. N. N. Akhmediev, J. M. Soto-Crespo, S. T. Cundiff, B. C. Collings, and W. H. Knox, "Phase locking and periodic evolution of solitons in passively mode-locked fiber lasers with a semiconductor saturable absorber," *Opt. Lett.* **23**(11), 852–854 (1998).
10. J. M. Soto-Crespo, N. N. Akhmediev, B. C. Collings, S. T. Cundiff, K. Bergman, and W. H. Knox, "Polarization-locked temporal vector solitons in a fiber laser: theory," *J. Opt. Soc. Am. B* **17**(3), 366–372 (2000).
11. S. T. Cundiff, B. C. Collings, N. N. Akhmediev, J. M. Soto-Crespo, K. Bergman, and W. H. Knox, "Observation of polarization-locked vector solitons in an optical fiber," *Phys. Rev. Lett.* **82**(20), 3988–3991 (1999).
12. B. C. Collings, S. T. Cundiff, N. N. Akhmediev, J. M. Soto-Crespo, K. Bergman, and W. H. Knox, "Polarization-locked temporal vector solitons in a fiber laser: experiment," *J. Opt. Soc. Am. B* **17**(3), 354–365 (2000).
13. D. Y. Tang, H. Zhang, L. M. Zhao, and X. Wu, "Observation of high-order polarization-locked vector solitons in a fiber laser," *Phys. Rev. Lett.* **101**(15), 153904 (2008).
14. R. Gumenyuk and O. G. Okhotnikov, "Temporal control of vector soliton bunching by slow/fast saturable absorption," *J. Opt. Soc. Am. B* **29**(1), 1–7 (2012).
15. H. Zhang, D. Y. Tang, L. M. Zhao, and H. Y. Tam, "Induced solitons formed by cross-polarization coupling in a birefringent cavity fiber laser," *Opt. Lett.* **33**(20), 2317–2319 (2008).
16. C. Mou, S. Sergeev, A. Rozhin, and S. Turistyn, "All-fiber polarization locked vector soliton laser using carbon nanotubes," *Opt. Lett.* **36**(19), 3831–3833 (2011).

17. J. H. Wong, K. Wu, H. H. Liu, Ch. Ouyang, H. Wang, S. Aditya, P. Shum, S. Fu, E. J. R. Kelleher, A. Chernov, and E. D. Obraztsova, "Vector solitons in a laser passively mode-locked by single-wall carbon nanotubes," *Opt. Commun.* **284**(7), 2007–2011 (2011).
 18. Ch. Tsao, *Optical fiber waveguide analysis* (Oxford University Press, New York, 1999).
 19. T. Tanemura and K. Kikuchi, "Circular-birefringence fiber for nonlinear optical signal processing," *J. Lightwave Technol.* **24**(11), 4108–4119 (2006).
 20. M. Midrio, S. Wabnitz, and P. Franco, "Perturbation theory for coupled nonlinear Schrödinger equations," *Phys. Rev. E Stat. Phys. Plasmas Fluids Relat. Interdiscip. Topics* **54**(5), 5743–5751 (1996).
 21. M. J. Ablowitz and H. Segur, *Solitons and the Inverse Scattering Transform* (Society for Industrial and Applied Mathematics, 1981).
 22. I. Mandelbaum, M. Bolshtyansky, T. F. Heinz, and A. R. H. Walker, "Method for measuring the Raman gain tensor in optical fibers," *J. Opt. Soc. Am. B* **23**(4), 621–627 (2006).
 23. J. Yang, "Classification of the solitary waves in coupled nonlinear Schrodinger equations," *Physica D* **108**(1-2), 92–112 (1997).
-

1. Introduction

Soliton propagation in optical fiber is often treated as a scalar problem, and the vector nature of light is ignored [1,2]. Common optical fibers, however, are randomly birefringent, and pulses traveling in them develop random polarization states upon propagation. The propagation of a pulse in a low birefringence fiber was considered for the first time in [3–5] using coupled nonlinear Schrödinger equations. It was shown that fractional pulses in each of the two polarizations trap each other and move together as one unit called vector soliton. The frequency of each pulse is shifted to compensate the difference in group velocities caused by birefringence. The experimental observation of vector solitons was reported in [6].

Initially the investigations were concentrated in the locking of group velocity; the phase velocity difference was ignored. However the phase difference between components determines the polarization of the pulse and this issue is very important, in particular for mode-locked fiber lasers. If the phase velocities of orthogonally polarized pulses are different, the polarization of the vector soliton changes along the fiber. If the components are locked in phase, then the state of polarization can be fixed along the fiber as well. These types of solution were the subject of investigation in [7]. The phase velocity locking was predicted theoretically, and independently the polarization locking was observed in [8] for an Er/Yb mode-locked laser, the results were recognized in [9] as a polarization locked vector soliton.

Investigation of polarization locked vector solitons is an especially important issue for mode-locked fiber lasers because polarization stability of lasers is highly desirable. Theoretical consideration of polarization locked vector solitons in the passive mode-locked laser was reported in [10]. Several observations of the polarization locked solitons in passive mode-locked lasers were reported using semiconductor saturable absorber, see for example [11–15], or carbon nanotubes [16,17].

Attention was given focused mainly on the vector solitons in linearly birefringent fibers; the effect of the Raman soliton self-frequency shift and circularly birefringent fibers, as far as we know, were never considered. However, fibers with circular birefringence, in particular twisted ones, may present advantages for laser applications. Fiber twist introduces circular birefringence and cancels random linear birefringence [18]. This makes the twisted fiber less sensitive to environmental conditions and provides new useful features for nonlinear applications [19].

In this paper we demonstrate that in a circularly birefringent fiber the cross-polarization Raman term leads to unidirectional energy transfer from the slow circularly polarized component to the fast one. The magnitude of this effect is determined by the product of birefringence and amplitudes of both polarization components. Thus, solitons with any initial polarization state will eventually evolve in a twisted fiber into stable circularly polarized ones. We demonstrate this effect numerically and make an analytic estimation of its magnitude using a perturbation theory for vector solitons [20].

2. Analytical consideration

The coupled equations that are used for the analysis were obtained from equations in the basis of the linear polarization [2]. In terms of the right and the left-polarized components $C^+(z,t)$, $C^-(z,t)$ the equations are:

$$i\partial_z C^+ + i\beta_1 \partial_t C^+ - \frac{\beta_2}{2} \partial_t^2 C^+ = -\frac{2}{3} \gamma (|C^+|^2 + \mu |C^-|^2) C^+ + \gamma T_R \left[\frac{1+\alpha}{2} \partial_t (|C^+|^2 + |C^-|^2) C^+ + (1-\alpha) \partial_t (\text{Re}(C^+ C^{*-})) C^+ \right], \quad (1)$$

$$i\partial_z C^- - i\beta_1 \partial_t C^- - \frac{\beta_2}{2} \partial_t^2 C^- = -\frac{2}{3} \gamma (|C^-|^2 + \mu |C^+|^2) C^- + \gamma T_R \left[\frac{1+\alpha}{2} \partial_t (|C^+|^2 + |C^-|^2) C^- + (1-\alpha) \partial_t (\text{Re}(C^+ C^{*-})) C^- \right]. \quad (2)$$

Here $2\beta_1$ is the group velocity difference between right and left circularly polarized components; β_2 is the second order dispersion, which is negative for soliton formation regime, γ is the Kerr nonlinear coefficient and T_R is the characteristic Raman time. The first term to the right-hand side describes the vectorial Kerr nonlinearity, and the second one the contribution of the Raman effect. For a basis of two circular polarizations the parameter μ of a cross-phase modulation is 2. For a special relation between linear and circular birefringence, μ can be done equal to 1 in the basis of elliptical eigenmodes: this corresponds to the analytically important Manakov problem, which permits IST (Inverse Scattering Transform) method application and has exact solitonic solutions [21]. The coefficient α describes the cross-polarization influence in the Raman term. There is some discussion in literature about its magnitude. For frequencies close to the Raman amplification maximum $\alpha \ll 1$, and for Raman amplification studies it is often taken equal to zero. However, the cross-phase modulation term is frequency-dependent, and for small frequencies, which are important here, the value of α , according to measurements of Ref [22], is close to 0.3.

It is well established, that the initial smooth pulse under the evolution described by Eqs. (1) and (2) tends to split in a number of soliton-like pulses, similarly to the scalar and Manakov cases. For a general situation two polarization components in the exact self-similar analytic solutions without the Raman term have different phase velocities [23]. Such solutions do not demonstrate energy transfer between polarization components. We observed the energy transfer between components numerically if both nonzero circular birefringence and the Raman term are taken into account. To clarify the origin of the effect and its dependence on pulse and fiber parameters we perform the transformation of Eqs. (1) and (2), which reduces them to a form of perturbed Manakov task [20] (we use the notation of this paper):

$$i\partial_z U + \frac{1}{2} \partial_T^2 U + (|U|^2 + |V|^2)U = iR_U, \quad (3)$$

$$i\partial_z V + \frac{1}{2} \partial_T^2 V + (|U|^2 + |V|^2)V = iR_V. \quad (4)$$

Here the scaled time is $T = t|\beta_2|^{-1/2}$, $Z = z$, and scaled amplitudes are $U = C^+ \gamma^{1/2} \exp(i\beta^2 Z/2 + i\beta T)$ and $V = C^- \gamma^{1/2} \exp(i\beta^2 Z/2 - i\beta T)$, with $\beta = \beta_1 \beta_2^{-1/2}$.

The difference with the integrable Manakov case and the Raman term are both considered as a perturbation, R_U, R_V and moved to a right-hand side of Eqs. (3) and (4)

$$R_U = -i \left[\frac{1}{3} (|U|^2 - |V|^2)U + T_R |\beta_2|^{-1/2} \left(\frac{1}{2} \partial_T (|U|^2 + |V|^2)U + \partial_T (\text{Re}(UV^* \exp(-2i\beta T)))V \exp(2i\beta T) \right) \right], \quad (5)$$

$$R_V = -i \left[\frac{1}{3} (|V|^2 - |U|^2)V + T_R |\beta_2|^{-1/2} \left(\frac{1}{2} \partial_T (|U|^2 + |V|^2)V + \partial_T (\text{Re}(UV^* \exp(2i\beta T)))V \exp(-2i\beta T) \right) \right]. \quad (6)$$

After recasting Eqs. (1) and (2) in the form of Eqs. (3) and (4), the perturbative analysis can be done according to the results of [20]. For this purpose the one-soliton solution of Manakov equation is taken:

$$U = 2\nu \cos(\theta) \operatorname{sech}[2\nu(T - \xi)] \exp[i2k(T - \xi) + i\delta_U], \quad (7)$$

$$V = 2\nu \sin(\theta) \operatorname{sech}[2\nu(T - \xi)] \exp[i2k(T - \xi) + i\delta_V]. \quad (8)$$

Were $\theta, \xi, \delta_U, \delta_V$ are regarded as Z -dependent.

We are only interested here in terms affecting the polarization parameter θ . To the first approximation in perturbation, the corresponding evolution equation is given by Eq. (7) of Ref [20]:

$$\frac{d\theta(Z)}{dZ} = \frac{1}{4\nu} \operatorname{Re} \int [\cos(\theta) R_V \exp(-i2\kappa(T - \xi) - i\delta_V) - \sin(\theta) R_U \exp(-i2\kappa(T - \xi) - i\delta_U)] \cosh^{-1}(x) dx \quad (9)$$

with $x = 2\nu(T - \xi)$.

The right-hand side is estimated for the nonperturbed solution given by Eqs. (7) and (8). Assuming that there is a phase velocity difference between two polarization components, the only perturbative term affecting the intensity transfer between polarization components is due to the derivative $\partial_T \exp(\pm 2i\beta T)$ in the last terms of Eqs. (5) and (6). This contribution is $-T_R \beta_1 |\beta_2|^{-1} |V|^2 U (1 - \alpha)$ in R_U , and $+T_R \beta_1 |\beta_2|^{-1} |U|^2 V (1 - \alpha)$ in R_V . Using these expressions in Eq. (9), the integration is easily performed.

Converting back to the solution of Eqs. (1) and (2), we obtain that, if the vector soliton can be approximated along propagation by the form (not taking into account phases)

$$|C^+| \sim A \cos(\theta) \operatorname{sech}[A |\beta_2|^{-1/2} (t - t_0)], \quad (10)$$

$$|C^-| \sim A \sin(\theta) \operatorname{sech}[A |\beta_2|^{-1/2} (t - t_0)], \quad (11)$$

where A^2 is total power of the soliton. The z -evolution of θ is approximated by:

$$\frac{d\theta(z)}{dz} = \frac{2(1 - \alpha)}{3} \gamma A^2 \frac{T_R \beta_1}{|\beta_2|} \sin(\theta) \cos(\theta). \quad (12)$$

Equation (12) is easily integrated:

$$\frac{|C^-(z)|}{|C^+(z)|} = \tan(\theta(z)) = \tan(\theta(0)) \exp\left(\frac{2(1 - \alpha)}{3} \gamma A^2 \frac{T_R \beta_1}{|\beta_2|} z\right). \quad (13)$$

It can be seen from Eq. (13) that depending on the sign of β_1 the Raman term asymptotically transfers energy to one or another polarization component. The initial pulse with a fast polarization is stable: a perturbation with the orthogonal circular polarization exponentially diminishes. If the initial polarization is opposite, an initial perturbation with the orthogonal polarization exponentially grows. Thus, in a fiber with random birefringence one can expect random output soliton polarization state after long enough propagation. But for a twisted (circularly birefringent) fiber, the fast circular polarization component is stabilized by a cross-Raman term.

For the perturbation analysis we have taken Manakov equations, and the difference between Eqs. (1) and (2); and the Manakov case was considered as a perturbation. Strictly

speaking, in the perturbation term $\frac{1}{3}(|U|^2 - |V|^2)U$ in R_U , and in the corresponding term of R_V there is no small parameter, except if $|U|^2 \approx |V|^2$.

Because of the absence of the truly small parameter, the exactitude of the above approximations is quite difficult to control, thus it has to be confirmed numerically. As we show in the next section, Eq. (12) gives a reasonable estimation of the numerical results. The perturbation theory using a Lagrangian approach can be written for the non-Manakov case as well, but no simple closed analytic expressions exist in that case for self-similar solutions and, consequently, there is no simple analog for Eq. (12).

3. Numerical calculations

We solved Eqs. (1) and (2) using a split-step Fourier method. The calculations were made for a fiber nonlinearity of 1.6 /W-km, $\beta_2 = 25$ ps²/km, and $\beta_1 = 1$ ps/km or $\beta_1 = 10$ ps/km. The circular birefringence $\beta_1 = 1$ ps/km corresponds to a standard fiber twisted by approximately 6 turns per meter. For the Raman effect we used $T_R = 3$ fs [2] and $\alpha = 0.3$ [22]. The pulse shape of the vector soliton is generally not known exactly. Therefore to generate the vector soliton we introduced to the fiber a 40 W Gaussian pulse with duration at 1/e level equal to 60 ps with a Gaussian noise. The pulse breaks into solitons at a distance of approximately 1 km. After the formation of solitons we isolated the highest one, and used it as an initial pulse. The power ratio between the circularly-right and left components is calculated along the propagation path in the fiber. This procedure gives the dependence of the angle θ on z . The ellipticity of the solitons resulting from the pulse break-up process is distributed randomly around the ellipticity of the initial pulse. The change of ellipticity of the input pulse allows the change of ellipticity of the soliton. However the generation of the solitons with exactly specified ellipticity was impossible. We changed the polarization of the initial pulse from linear, $\theta = \pi/4$, to nearly circular, $\theta = 0.1\pi/4$. The power of the resulting solitons varied randomly in the range 10 to 15 times higher than the power of the initial pulse. An example of the ratio between powers of the circularly left- and right polarized components upon propagation is presented in the Fig. 1. The initial pulse had a linear polarization. The solid lines show the results of numerical calculations; the dashed lines show the results obtained by Eq. (13) where we used soliton power and initial ellipticity obtained from numerical calculation.

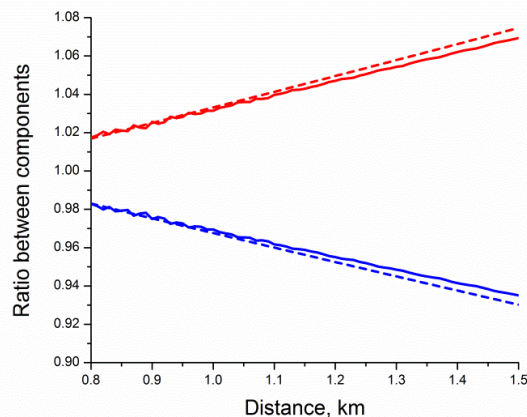


Fig. 1. Ratio between powers of the left- and right-circularly polarized components. Red and blue lines correspond to the fast and slow left circularly polarized component; solid lines – numerical, dashed lines – calculated using Eq. (13).

The left-circularly polarized component was the fast one for the result shown by the red line and the slow one for the result shown by the blue line. To switch the fast and low components we were changing the sign of β_1 . It is seen that, as it follows from Eq. (12), the energy is transferred from the slow component to the fast one. As we can see from the Fig. 1, the effect is not big for the typical experimental conditions used for calculations so the solution of Eq. (13) can be approximated by linear dependence at relatively short distances. Equation (13) gives results very similar to numerical ones. To verify the asymptotic approximation of vector soliton to circularly polarized one we used $\beta_1 = 10$ ps/km, the value which is difficult to achieve experimentally by twist, but helps to compare numerical and analytical approaches.

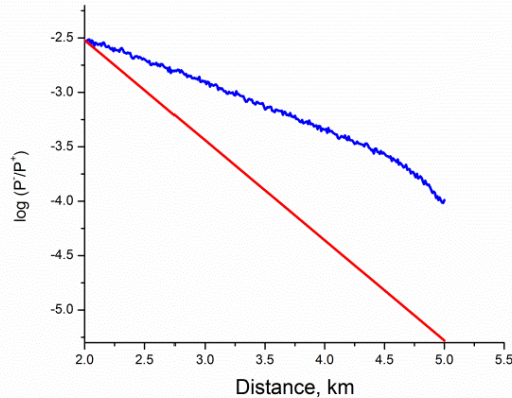


Fig. 2. An asymptotic approximation of the soliton polarization to the circular; the blue line - numerical, the red line - Eq. (13).

Figure 2 shows in logarithmic scale the ratio between powers of left (slow) and right (fast) circularly polarized components when an elliptically polarized input pulse with a power ratio between left- and right-circularly polarized components equal to 0.025 is used. In this case the polarization of the soliton generated in the pulse break-up process is much closer to the circular polarization than the input pulse. We can see that the polarization exponentially approaches the right-circular polarization (fast component). The dependence deviates from the exponential dependence only for very low values of the left-circularly polarized component, 40 dB below the right-circularly polarized component. This deviation may appear probably due to the exactitude of numerical approximation and non-solitonic part of the pulse. The analytical approximation in this case differs from the numerical more substantially than in the case shown in Fig. 1. It can be expected because the parameter which we used as small parameter in our approximation gets smaller when the polarization is approaching to the linear one. However in spite of quite coarse approximation used to derive Eq. (12) even for polarizations very close to the circular one analytics gives reasonably good order of value of the energy transfer.

For relatively short distances the dependence $\theta(z)$ can be considered as linear. In Fig. 3 we compare for different ellipticities the slopes of the dependence $\theta(z)$ calculated numerically and using Eq. (13). The value $\theta = 0.78$ corresponds to linear polarization; the value $\theta = 0$ corresponds to the circularly polarized soliton. According to our approximation it can be expected that the correspondence between analytical approximation and numerical results tends to be better when polarization of solitons is approaching to linear one.

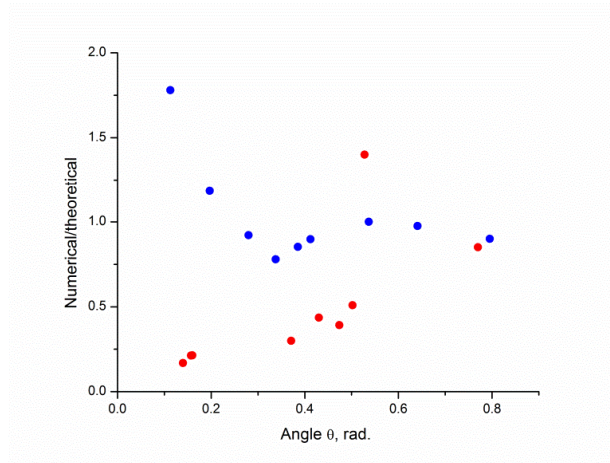


Fig. 3. Ratio between numerical and theoretical slopes of the dependence $\theta(z)$.

The results shown in Fig. 3 corroborate this. For polarization close to linear ($\theta \approx 0.78$) the ratio between the slopes calculated analytically and numerically is close to the one, however for angles θ less than approximately 0.2 the ratio deviates substantially from the one. Red circles show the slope of $\theta(z)$ when the polarization approaches the fast circular polarization, the polarization which is expected to be stable. For this case Eq. (12) gives faster energy transfer than numerical calculations. Blue circles correspond to the polarization close the slow circular polarization, unstable polarization. In this case the analytical approximation gives slower energy transfer than the numerical calculations. However, even for polarization close to circular Eq. (12) gives a good qualitative idea of the energy transfer in question.

4. Conclusions

We demonstrated numerically and by analytical analysis that in a fiber with circular birefringence the joint action of the Raman self-frequency shift and group velocity difference between left- and right-circularly polarized components results in the unidirectional energy transfer from the slow circularly polarized component to the fast one. The magnitude of this effect is determined by the product of birefringence and amplitudes of both polarization components. Thus, solitons with any initial polarization state will eventually evolve into the stable circularly polarized ones.

Acknowledgment

This work was supported by the CONACYT project 130966.